

19. THE PETROLOGY AND ⁴⁰AR/³⁹AR AGE OF THOLEIITIC BASALT RECOVERED FROM HOLE 907A, ICELAND PLATEAU¹

Linda L. Davis² and William C. McIntosh³

ABSTRACT

Crystalline rock recovered from the Iceland Plateau at 69°14.989'N, 12°41.894'W in August 1993, is tholeiitic basalt. Pillow structures are well defined by glassy rims grading into vesicular rinds and aphyric interiors. Some plagioclase and augite microphenocrysts are present, and olivine may have been. Pigeonite is found in cores of some augite. Major- and trace-element abundances vary indicating magma-mixing, but the nature of the magma-mixing is not known. Trace-element ratios also vary, sometimes greatly, indicating that the "mixed magmas" may be magmas derived from different depths in a melting column, as has been proposed by other workers. The rocks differ from many typical MORB samples in that they are relatively evolved (mg = 46); however, they are strikingly similar to the majority of basalt glasses from the Kolbeinsey Ridge. Iceland Plateau basalts are T-MORBs, transitional to N-MORB and E-MORB with (La/Sm)_n 0.68–0.72, Zr/Nb < 20, and a range of major- and trace-element abundances that also clearly span the gap between average N-MORB and average E-MORB. An ⁴⁰Ar/³⁹Ar age of 13.2 ± 0.3 Ma from groundmass concentrates is an accurate but possibly imprecise age.

INTRODUCTION

Site 907 of the Ocean Drilling Program (ODP) Leg 151 was drilled on the southern Iceland Plateau, an area of shallow seafloor extending from Iceland to about 70°N, and west to east from Greenland to the Jan Mayen Ridge. Site 907 sits east of the present spreading ridge, the Kolbeinsey Ridge, and west of a feature that has been considered by some to be an extinct spreading axis. Vogt et al. (1980) considered this ridge to be the east flank of Kolbeinsey Ridge rather than an extinct spreading axis, based on morphology and magnetic anomalies. Crystalline rock, or basement, was originally slated to be drilled only in the Fram Strait and the Yermak Plateau areas; however, basalt was drilled at Site 907, the first site of Leg 151. No other crystalline rock, besides ice-rafted debris or "dropstones," was recovered during Leg 151. Site 907 sits on a shallow part of the Iceland Plateau, on ocean crust that was thought to be approximately 22–24 Ma because of its proximity to magnetic Anomaly 6B. About 8 m of basalt was drilled, but only 5 m was recovered. The recovered basalt cores were divided into 12 cooling units, which are individual basalt pillows with tops, bottoms, and sides defined by glassy, vesicle-rich chill zones. We have characterized the textures, composition, and age of the basalts drilled, but it is important to remember that only one hole was drilled so there is little three-dimensional control. Seismic data show that the basalt came from a very smooth reflector that may not represent acoustic basement (Shipboard Scientific Party, 1995). This basalt layer may be the same as the layer drilled at Deep Sea Drilling Project (DSDP) Site 348 even though pillow structures are very well defined at Site 907, and no pillows were found at Site 348 (Talwani, Udintsev, et al., 1976). Although many workers have studied the ocean floor in this area, there are few drill sites on the Iceland Plateau where basalt has been recovered (e.g., Talwani, Udintsev, et al., 1976; Wood et al., 1979; Schilling et al., 1983; Elliot et al., 1991;

Mertz et al., 1991; Fram and Leshner, 1993; Devey et al., 1994). The chemistry and age of the basalt pillows at Site 907 may be applicable to regional questions regarding the Iceland Plateau basement. We are not convinced, however, that these pillows are "basement." Because we do not know the source of the flow(s) if they are not "basement," it is necessary to use caution if applying the following data to the Iceland Plateau as a region.

ANALYTICAL TECHNIQUES

Basalt core was examined, described, sampled, and analyzed aboard the *JOIDES Resolution* during Leg 151. Polished thin sections were made aboard ship, as were fused disks for X-ray fluorescence (XRF) analyses. Core and thin section descriptions can be found in Shipboard Scientific Party (1995) along with photographs of core and photomicrographs of thin sections.

Microprobe Analysis

Polished thin sections made aboard ship were further analyzed petrographically at the University of Texas Department of Geological Sciences. Pyroxene, plagioclase, and ilmenite compositions are reported here. A JEOL 733 electron microprobe operated at 15 kv was used with sample currents of 10–15 nA on brass, beam diameters of up to 10 μm, and counting times of 10–35 s. Counting was terminated if a precision of 0.30–0.50 relative percent (1σ) was attained. Natural and synthetic standards were used for the following elements: Glass K412 (Si), Amelia albite (Na), titanium-doped diopside glass (Ca), fayalite (Fe), orthoclase (K), BaO silica glass (Ba), anorthite (An₁₀₀, Al), synthetic enstatite (Mg), Mn garnet (Mn), and IM-8 chromite (Cr). Precision estimates based on the standard deviation of replicate analyses of secondary standards were as follows: Si = 0.1–0.7; Al = 0.1–0.3; T = 0.02–0.3; Cr = 0.02–0.04; Fe = 0.1–0.7; Mn = 0.02; Mg = 0.17–0.44; Ca = 0.03–0.3; Na = 0.03–0.09; and K = 0.19–0.24.

X-ray Fluorescence Analysis

Rock powders were ground aboard the *JOIDES Resolution* from core samples that were cut with a steel saw and sonicated in distilled

¹Thiede, J., Myhre, A.M., Firth, J.V., Johnson, G.L., and Ruddiman, W.F. (Eds.), 1996. *Proc. ODP, Sci. Results, 151*: College Station, TX (Ocean Drilling Program).

²Department of Geological Sciences, The University of Texas, Austin, Texas 78712, U.S.A. Present address: Department of Geology, Idaho State University, Pocatello, Idaho 83209-8072, U.S.A. davilin2@fs.isu.edu

³New Mexico Bureau of Mines and Mineral Resources, Socorro, New Mexico 87801, U.S.A.

water. Grinding and crushing methods employed aboard the *JOIDES Resolution* are described in Shipboard Scientific Party (1992). Fused glass disks were made from powders and analyzed by XRF for major elements only. Volatile content for each sample was determined by loss on ignition (LOI) aboard ship; no sample had more than 0.70 wt% LOI.

International standard BIR-1 was analyzed with the Site 907 basalts as a check on precision and accuracy (Shipboard Scientific Party, 1992). Major oxides determined aboard ship for BIR-1 were in excellent agreement with recommended values with the exception of SiO₂. Precision based upon the standard deviation of replicate analyses of BIR-1 was: SiO₂ = 0.02; TiO₂ and Al₂O₃ = 0.01; Fe₂O₃ = 0.06; MgO and CaO = 0.04 and 0.06; and MnO, K₂O, Na₂O, and P₂O₅ = 0.00. SiO₂ values for the BIR samples analyzed as unknowns were consistently 0.4 wt% lower than the recommended value. For this reason, splits of the same samples were analyzed a second time by XRF in a different laboratory.

XRF analyses of sample splits analyzed at the GeoAnalytical Laboratory, Department of Geology, Washington State University, were in excellent agreement with the first XRF data set. Estimates of precision of these analyses are very good but variable. They are available in Hooper et al. (1993), along with analytical procedures. Trace elements were also determined by the GeoAnalytical Laboratory.

The major oxide data presented herein are the average of the analyses from the two different laboratories. The trace elements determined by XRF (i.e., V, Ni, Cu, Zn, Ga, Rb, Sr, Y, Zr, Nb, and Pb) are from the single analysis done by GeoAnalytical Laboratories.

Instrumental Neutron Activation Analysis

Rock powders ground to 100–200 mesh with a ball mill in a ceramic vessel at the University of Texas, Department of Geological Sciences, were sent to XRAL Activation Services, Inc. in Ann Arbor, Michigan, for instrumental neutron activation analysis (INAA). Prior to grinding, rock cores had been washed and sonicated in distilled water after having been cut with a steel saw on board. The cut core was then chipped to pea-size on a hardened steel plate with a rock hammer before grinding in a SPEX ball mill. Rock powders are not splits of the powders analyzed by XRF; ideally, they would have been, but the amount of sample taken at any particular depth in the core is restricted. These samples were taken as close to the other samples used for thin sections and XRF as possible and certainly within the same pillows. One secondary standard previously analyzed by INAA sent as an "unknown" was analyzed with the Site 907 basalt samples along with a control sample (NIST-278, obsidian). The analysis of NIST-278 compares favorably with the recommended or certified concentrations, and the analysis of the secondary standard submitted as an unknown also compares favorably with a previous INAA analysis, with the exception of La. La determined by NIST-278 was 33.9 ppm whereas the recommended or certified value is 33 ppm; therefore, La values here are probably good. Ce, Nd, and Sm are fission-product corrected based on the amount of uranium in the sample, which is almost negligible here.

⁴⁰Ar/³⁹Ar Procedures

Groundmass concentrates were prepared by crushing and sieving the samples to 250–400 μm, followed by ultrasonic cleaning in dilute (7%) hydrochloric acid, followed by hand-picking to remove fragments containing visible phenocrysts. Aliquots (30–38 mg) of each groundmass concentrate were packaged with alternating flux monitors of Fish Canyon Tuff sanidine (27.84 Ma, relative to MMhb-1 hornblende at 520.4 Ma; Samson and Alexander, 1987) and irradiated for 5 hours in the L 67 position of the Ford reactor at the University of Michigan.

⁴⁰Ar/³⁹Ar analyses were performed at the New Mexico Geochronology Research Laboratory at the New Mexico Institute of Mining

and Technology. This facility includes an MAT215–50 mass spectrometer attached to a fully automated all-metal argon extraction system equipped with a 10-watt CO₂ laser and a low blank resistance furnace. The neutron flux values (J-values) within irradiation packages were determined to a precision of ±0.25% by averaging laser-fusion results of four subsamples (each 1–4 crystals, ~1 mg) of each sanidine monitor. Groundmass concentrates were analyzed by incremental step-heating in the resistance furnace, using twelve 10-min heating steps ranging from 500 to 1650°C. Reactive gasses were removed using SAES AP-10 and GP-50 getters before expansion into the mass spectrometer. Extraction line blanks during these analyses ranged from 5 × 10⁻¹⁶ to 2 × 10⁻¹⁵ moles ⁴⁰Ar and 6 × 10⁻¹⁸ to 1 × 10⁻¹⁷ moles ³⁶Ar.

MINERALOGY

Composition of microphenocrysts and groundmass phases determined by electron microprobe is discussed here, but is preceded by a brief summary of the petrography of the basalts. The basalts from Site 907 are pillow basalts with glassy rinds that grade into a zone rich in vesicles and amygdules, and then into aphyric interiors (Shipboard Scientific Party, 1995). Plagioclase, pyroxene, and altered olivine microphenocrysts are not larger than 2.0 mm and usually less than 1.5 mm. Volumetrically, microphenocrysts make up between 5% and 20% of the pillows. Detailed thin section and macroscopic core descriptions were completed during the cruise and are reported in Myhre, Thiede, Firth, et al. (1995). Textures in the basalts range from vitrophytic to subophitic, with amygdules, microphenocrysts, and glomerocrysts (Fig. 1; fig. 23 in Shipboard Scientific Party, 1995). Groundmass is typically quenched with skeletal grains and sheaves or blades of plagioclase, pyroxene, and ilmenite (Fig. 1). No spinel or unaltered olivine were found; what may have been olivine is present in the groundmass as a mixture of brown minerals, but euhedral olivine outlines are rare. Glass was possibly present in pillow interiors; however, if so, it has been replaced by a brown fibrous material. The pillow rims that macroscopically appear glassy are dark brown, turbid, and mostly devitrified in thin section (fig. 23B in Shipboard Scientific Party, 1995).

Plagioclase

Labradorite with some bytownite (An_{56–74}) is found as euhedral microphenocrysts often intergrown with clinopyroxene and pigeonite, as skeletal sheaves or blades in the groundmass, and is optically intergrown with clinopyroxene (Table 1; Figs. 1, 2). Grains are uniformly poor in the orthoclase component. Although the number of analyses are few, they are probably representative of most or all of the feldspar in the sampled core.

Compositional differences related to depth or chemical evolution of the parent magmas are not evident, but this may be related to the number of grains analyzed (approximately 55) or to the difficulty in obtaining good analyses of groundmass feldspar, which is related to their small size. The larger microphenocrysts are slightly more calcic than the smaller microphenocrysts and groundmass plagioclase (Table 1). An increase in anorthite content in the plagioclase is not seen with depth. Microphenocrysts are zoned, but while the core of a given grain is richer in anorthite content than one rim, the other rim may have approximately the same anorthite content as the core (Table 1). Therefore, the zoning does not appear to be concentric and is certainly not oscillatory.

Pyroxene

Resorbed and euhedral clinopyroxene microphenocrysts are generally zoned and are often glomerocrystic with plagioclase (Fig. 1). In the groundmass, pyroxene is either lath-like or plumose and sheaf-

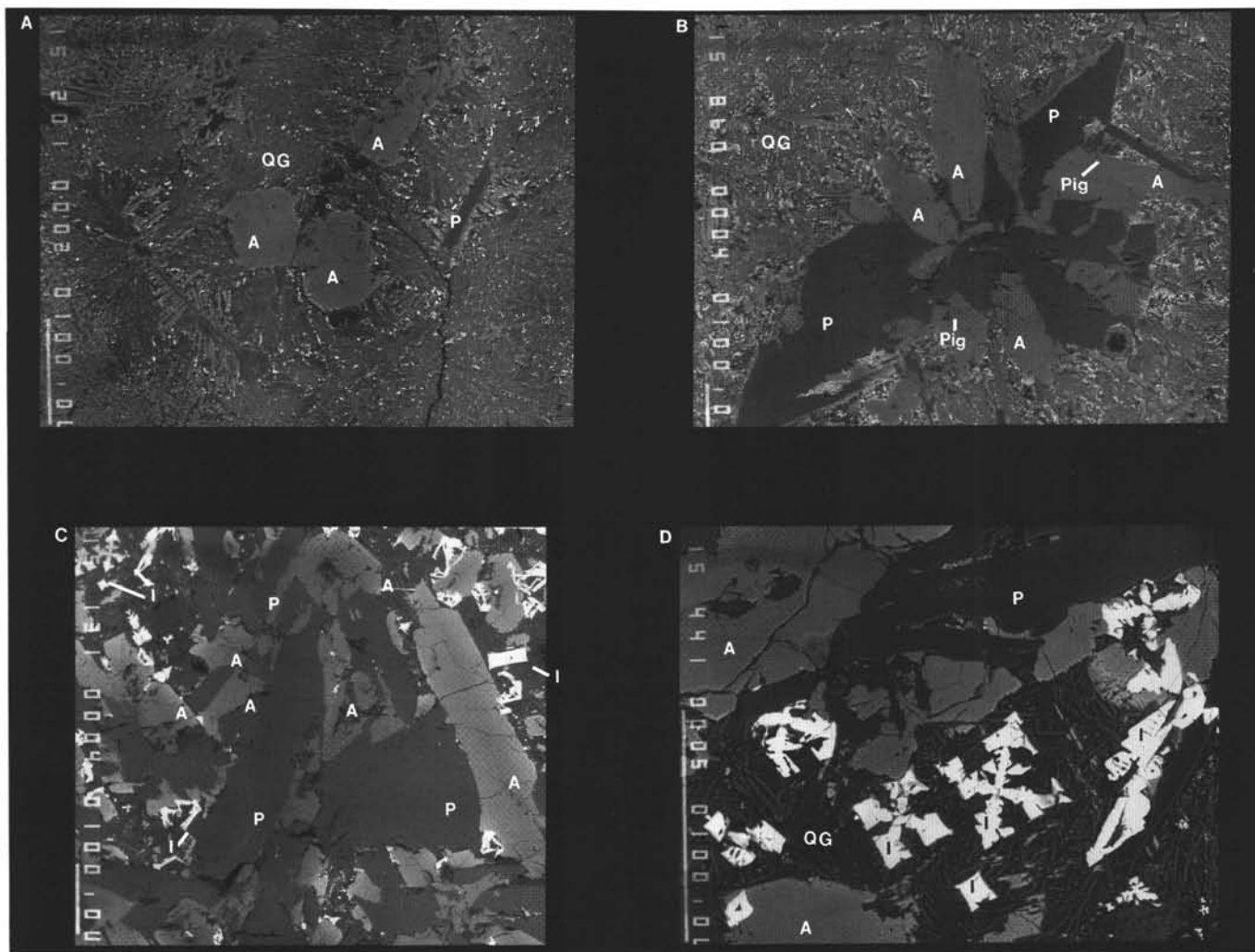


Figure 1. Back-scattered electron (BSE) photographs. Scale bar of 100 μm is shown to the left of each photograph. **A.** Sample 151-907A-25X-1, 108–111 cm. Quenched groundmass (QG) of pyroxene (medium gray), plagioclase (P) (dark gray), and iron oxides, mostly or all ilmenite (bright white specks) with microphenocrysts of plagioclase and zoned pyroxene (A). **B.** Sample 151-907A-26X-2, 6–11 cm. Euohedral plagioclase (P) microphenocryst (dark gray) intergrown with augite (A) and pigeonite (Pig) (lighter gray). Pigeonite is very difficult to see, but the subtly darker gray within the clinopyroxene grains is the pigeonite. Groundmass is the same as in A. **C.** Sample 151-907A-26X-1, 85–89 cm. Clinopyroxene (A) and plagioclase (P) coarsely intergrown, skeletal ilmenite (I), and a quenched groundmass. **D.** Sample 151-907A-26X-1, 85–89 cm, enlargement of top left-hand corner of C. Skeletal ilmenite (I) in quenched groundmass (QG) near clinopyroxene (A) and plagioclase (P) intergrowth.

like. In places, it is altered to a cryptocrystalline material, perhaps an amphibole, but the composition of the alteration product(s) is undetermined.

Pyroxene compositions range from augite to subcalcic pyroxene or pigeonite (Table 2; Fig. 3). These pyroxenes follow a trend characteristic of pyroxenes in quenched volcanic rocks as discussed by Muir and Tilley (1964). Pigeonite is not discernible in thin section and is only barely distinguishable from augite in back-scattered electron images (Fig. 1B). Most of the augites have iron-rich rims as expected, but cores of, or zones central to, some of the grains are actually pigeonite (Table 2; Fig. 1). Subcalcic pyroxene or pigeonite (e.g., $\text{En}_{69}\text{Fs}_{23}\text{Wo}_8$) was found in two samples (Fig. 3; Table 2) and is probably in many of the basalt pillows at Site 907, but it is perhaps too difficult to distinguish when weighed against the time needed to find the grains by microprobe analysis. Within each sample analyzed, pyroxene grains range mostly in Wo content, but a range in En–Fs is also seen (Fig. 3). The compositional ranges of different samples overlap such that no pattern is evident.

Structural formulas calculated from microprobe analyses confirm that the analyses are acceptable and that the pyroxenes are stoichiometric (Table 2). Deficiencies in the tetrahedral sites are filled by adding about 0.1 Al to Si to make an ideal 2. Cations were normalized to 4 and Fe^{3+} was thereby calculated using the summed oxygen difference from 6. If Al^{VI} , Fe^{3+} , Cr^{3+} , Ti, Mg, Fe^{2+} , and Mn are put into the M1 cation site, then the M1 cation sum is approximately 1.3 for all clinopyroxenes, so all Mn and most Fe^{2+} must be put into the M2 cation site to satisfy criteria outlined by Robinson (1980) for pyroxene structure.

Ilmenite

Ilmenite is generally skeletal with a wide variety of shapes (Fig. 1) and is only rarely intergrown with pyroxene. There appear to be two generations present, with most of the grains so fine grained that analysis by electron microprobe is not possible, even with a minimum beam size. However, it is possible to analyze the flared tip ends

Table 1. Selected electron microprobe analyses of feldspars in basalt from Site 907.

151-907A-:	26X-1,	26X-1,	26X-1,	25X-1,	25X-1,	25X-1,	25X-1,	25X-1,	25X-1,	25X-1,	25X-1,	25X-1,	26X-2,	26X-2,	26X-2,
Interval (cm):	85-89	85-89	85-89	108-119	108-119	108-119	108-119	81-84	81-84	81-84	81-84	81-84	6-11	6-11	6-11
SiO ₂	52.7	53.2	54.0	51.4	51.7	50.5	51.4	52.0	52.5	54.9	51.6	50.2	52.3	53.0	51.8
Al ₂ O ₃	29.4	29.0	28.2	29.5	29.2	30.4	29.5	29.5	29.0	26.9	29.0	30.3	29.2	28.8	29.9
Fe ₂ O ₃	1.04	1.08	1.26	0.84	0.94	0.80	0.96	1.02	0.99	1.27	0.76	0.9	0.93	0.97	0.84
CaO	13.5	13.0	12.3	13.4	13.7	14.5	14.0	13.2	13.1	11.0	13.8	14.8	13.4	13.8	14.2
Na ₂ O	3.65	3.91	4.41	3.40	3.31	2.85	3.27	3.45	3.75	4.67	3.32	2.85	3.29	3.51	3.10
K ₂ O	0.03	0.04	0.03	0.06	0.10	0.06	0.02	0.04	0.02	0.08	0.02	0.00	0.04	0.02	0.03
Total	100.3	100.2	100.2	98.6	99.0	99.1	99.2	99.2	99.3	98.8	98.5	99.1	99.2	100.1	99.9
Si	2.389	2.409	2.443	2.369	2.376	2.322	2.360	2.382	2.399	2.507	2.375	2.313	2.393	2.407	2.358
Al	1.569	1.546	1.507	1.603	1.581	1.647	1.596	1.589	1.563	1.449	1.576	1.646	1.575	1.541	1.605
Fe ³⁺	0.035	0.037	0.043	0.029	0.032	0.028	0.033	0.035	0.034	0.044	0.026	0.031	0.032	0.033	0.029
Ca	0.655	0.633	0.596	0.660	0.676	0.715	0.689	0.645	0.641	0.538	0.679	0.73	0.656	0.670	0.695
Na	0.321	0.343	0.387	0.304	0.295	0.254	0.291	0.306	0.333	0.413	0.296	0.255	0.292	0.309	0.274
K	0.002	0.002	0.002	0.004	0.006	0.003	0.001	0.003	0.001	0.005	0	0	0.002	0.001	0.002
Ab	32.8	35.1	39.3	31.4	30.2	26.1	29.7	32.1	34.2	43.2	30.4	25.9	30.7	31.6	28.2
An	67.0	64.7	60.5	68.2	69.2	73.5	70.2	67.7	65.8	56.3	69.6	74.1	69.1	68.3	71.6
Or	0.20	0.24	0.16	0.39	0.60	0.36	0.15	0.28	0.10	0.50	0.0	0.0	0.3	0.1	0.2
Description	r-	-c-	-r,	e ph	r-	c-	-r,	r-	-m-	-r,	c-	-c,	ph-	-sa ph,	ph r

Note: Symbols describing the physical nature of the grains are: c = core, r = rim, m = mantle, ph = phenocryst, e = euhedral, and sa = same. Dashes indicate the analysis is one in a series of the same grain. Cations normalized to 8 oxygens.

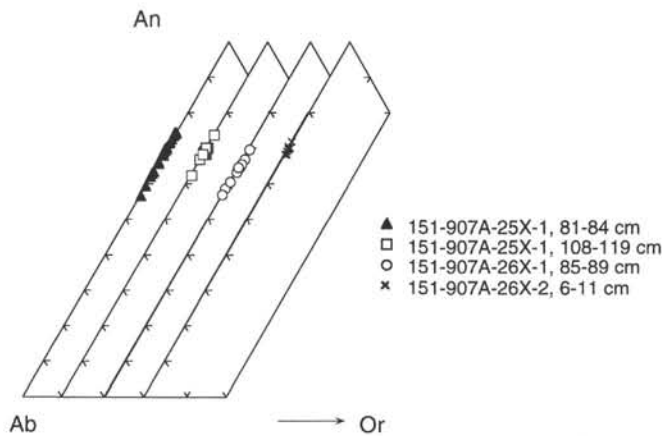


Figure 2. Plagioclase compositions determined by electron microprobe.

of some of the largest skeletal grains, which resemble crosses (Fig. 1C, D). Two analyses are shown in Table 2: the ilmenites are low in chromium with very low *cr'* (0.6–1.23), and also have low *mg* numbers (4.2–6.0).

WHOLE-ROCK GEOCHEMISTRY

Major-Element Compositions

Basalts recovered from Site 907 are tholeiitic, falling well within Macdonald and Katsura's (1964) tholeiitic field (Shipboard Scientific Party, 1995). The basalts have between 49 and 52 wt% SiO₂, yet have a much smaller range in MgO (6.2–7.1 wt% MgO, *mg* = 44–48) (Table 3; Fig. 4). Because SiO₂ variation is greater than that of MgO, variation diagrams are shown with SiO₂ as an abscissa rather than MgO, which is more typically used as a differentiation index to illustrate variations in basalt compositions (Fig. 5). SiO₂ in the basalts is high enough for them to be almost andesitic (Fig. 4). In part, normative analyses of the samples also reflect the high SiO₂, as most are quartz-normative tholeiites. Three basalt samples are olivine-normative, however, and all are hypersthene-normative (Table 3). The amount of normative quartz (*q*) or olivine (*ol*) present in these analyses is related to the amount of Fe₂O₃ present: here, Fe₂O₃ is set to be equal to 10% of FeO_(Total) as recommended by the Basaltic Volcanism

Study Project (1981). The relative percentages of *q* and *ol* will change depending upon the value of Fe₂O₃ chosen. So, although the basalts range from silica-oversaturated to just slightly silica-undersaturated, the difference between the samples may be more related to the assumption that Fe₂O₃ is 10% of FeO_(Total), rather than different lineages. Note that Units 5, 9, and 11, which are *ol*-normative, are also the three most mafic samples in the group.

Geochemical trends indicative of evolving compositions of a group of genetically related basalts are not well defined in the Iceland Plateau basalts (Fig. 5). The number of samples analyzed are few, however, and the range in each oxide is small, perhaps leading to scatter at the scales shown. Some of the oxides definitely decrease with increasing SiO₂, including Fe₂O_{3(T)}, CaO, MnO, and MgO. Other oxides that definitely increase with SiO₂ include TiO₂ and Al₂O₃.

Major element composition varies more or less consistently with depth in meters below seafloor (mbsf) (Fig. 6). The trends are in some cases well defined and are quite different above and below about 220 mbsf. Samples from near 220 mbsf were not analyzed geochemically due to severe alteration of the rocks, leaving a gap in the variation diagrams just where trends seem to dramatically change direction. With decreasing depth, between 224 and 220 mbsf, basalt pillows increase in Fe₂O_{3(T)}, CaO, and MnO and decrease in Al₂O₃, Na₂O, and TiO₂. At 220 mbsf, the patterns abruptly change and, from 220 mbsf to the top of the basalt pillows at about 216 mbsf, Fe₂O_{3(T)}, CaO, and MnO decrease with decreasing depth, and the other oxides, with the exception of P₂O₅, increase with decreasing depth.

Trace-Element Compositions

Trace-element variation in the basalts is almost as inconsistent as major-element variation (Table 4; Fig. 7). Y is perhaps the only element that varies smoothly with SiO₂ as an indicator of evolution of the melt(s) (Fig. 7). Some well-defined trends abruptly change direction, as illustrated by V and Eu (Fig. 7). Ga, Sc, and Lu tend to decrease with increasing SiO₂, and Ni, Sr, Zr, La, and Y seem to increase with increasing SiO₂. Few of these elements show good linear trends, and most could also be interpreted to be similar to Eu and V in that trends are different above and below 50% SiO₂. The lack of well-defined, straight-line trends may not be genetically related, but this may be due to the small number of samples and some trace-element abundances that do not greatly vary.

Trace-element variation seems to be considerably more coherent when normalized to chondrite or mid-ocean-ridge basalt (MORB) values (database of MORB values from Wheatley and Rock, 1988, comes mainly from Mid-Atlantic Ridge samples). Chondrite-normal-

Table 2. Selected electron microprobe analyses of pyroxenes and ilmenites in basalt from Site 907.

151-907A-:	26X-1,	26X-1,	25X-1,	25X-1,	26X-2,	26X-2,	26X-2,	26X-2,	26X-1,	25X-1,
Interval (cm):	85-89	85-89	81-84	81-84	6-11	6-11	6-11	6-11	85-89	81-84
SiO ₂	50.5	51.2	52.2	51.8	53.1	54.9	55.1	51.4	0.19	0.18
TiO ₂	0.83	0.81	0.42	0.64	0.45	0.18	0.19	0.65	20.4	21.2
Al ₂ O ₃	2.91	3.30	2.14	2.62	2.09	0.79	0.76	3.05	2.65	2.15
Cr ₂ O ₃	0.00	0.02	0.06	0.07	0.26	0.12	0.04	0.19	0.05	0.01
FeO*	16.5	11.8	9.69	12.6	11.0	15.4	14.7	9.51	70.1	68.2
MnO	0.29	0.29	0.23	0.32	0.26	0.40	0.45	0.21	0.43	0.47
MgO	15.1	16.3	17.8	19.0	18.5	24.4	25.1	15.5	0.43	0.63
CaO	14.2	17.0	17.3	12.8	15.1	4.86	4.19	19.6	0.11	0.09
Na ₂ O	0.19	0.20	0.19	0.14	0.17	0.05	0.05	0.23		
Total	100.4	100.9	100.0	100.0	100.9	101.1	100.5	100.2	94.4	92.9
Si	1.896	1.885	1.919	1.908	1.938	1.978	1.987	1.900	0.005	0.005
Ti	0.023	0.022	0.012	0.018	0.012	0.005	0.005	0.018	0.391	0.412
Al	1.286	0.143	0.093	0.114	0.090	0.034	0.032	0.133	0.080	0.066
Cr	0.000	0.0005	0.002	0.002	0.008	0.003	0.001	0.006	0.001	0.000
Fe ²⁺	0.470	0.306	0.240	0.346	0.322	0.464	0.444	0.252	0.365	0.374
Fe ³⁺	0.046	0.057	0.058	0.043	0.013	0.001	0.000	0.042	1.129	1.103
Mn	0.009	0.009	0.007	0.010	0.008	0.012	0.014	0.007	0.009	0.010
Mg	0.843	0.894	0.974	1.042	1.008	1.312	1.351	0.852	0.016	0.024
Ca	0.569	0.669	0.682	0.507	0.590	0.188	0.162	0.775	0.003	0.002
Na	0.014	0.014	0.013	0.010	0.012	0.004	0.004	0.017		
mg	64	74	80	75	76	74	75	77	4.2	6.0
cr'									1.23	0.60
New FeO	15.0	9.93	7.8	11.2	10.5			8.15	17.1	17.3
New Fe ₂ O ₃	1.65	2.05	2.1	1.55	0.46			1.51	58.9	56.6
New total	100.7	101.1	100.2	100.1	100.9			100.5	100.3	98.6
En	44.8	47.8	51.4	55.0	52.5	66.8	69.0	45.3		
Fs	25.0	16.3	12.6	18.2	16.8	23.6	22.7	13.4		
Wo	30.2	35.8	36.0	26.8	30.7	9.6	8.3	41.2		

Note: Cations are normalized to 4. mg = $100 \times \text{Mg}/(\text{Mg} + \text{Fe}^{2+})$. cr' = $100 \times \text{Cr}/(\text{Cr} + \text{Al})$.

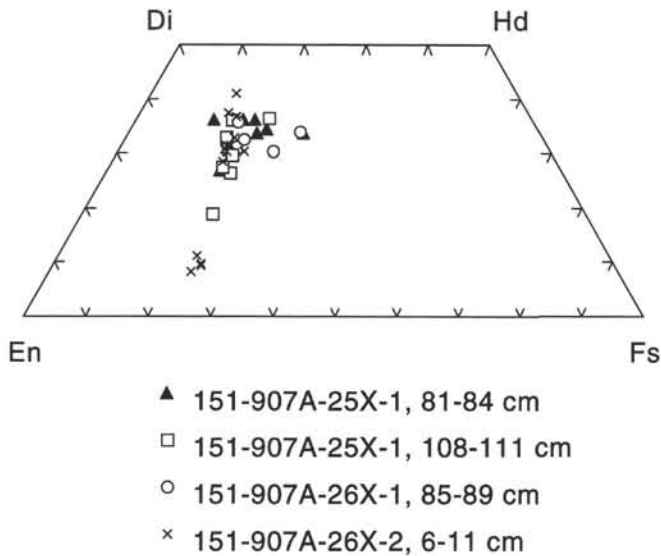


Figure 3. Pyroxene compositions determined by electron microprobe.

ized rare-earth element (REE) patterns are nearly flat, slightly enriched in REE over chondrite values, with normalized values between 10 and 25. The scale in Figure 8A is set to emphasize the slight depletion in the LREEs over the HREEs and to distinguish the Eu depletion relative to Sm or Gd for Units 2 and 5. When trace-element compositions of the Iceland Plateau basalts are normalized to MORB values for incompatibility plots, differences between Site 907 basalts and typical MORB are accentuated (Fig. 8B). Although some data is scarce in part because some samples were not analyzed by both XRF and INAA (thus, for example, no Rb data is available), compared to MORB all units have depletions in Cr, Ni, and Sr, and some units have slight depletions in K. It is difficult to substantiate, but it is like-

ly that the lack of coherency for some of the patterns on the incompatible element plots is due to analytical error, at least for Ce in Unit 9 (Fig. 8B). The spread in K may be real rather than an artifact of alteration or analytical error and will be discussed later. The incompatibility plots normalized to MORB in Figure 8B were normalized a second time so that K was set equal to 1 (Fig. 8C). Some of the inconsistencies in the patterns disappear, and the patterns are spread out so that their shapes can be better contrasted. Units 9 and 11 were not analyzed by INAA and therefore are missing some of the elements determined for the other units. This makes it difficult to determine whether Units 9 and 11 are actually different than the other units shown. In general, the shapes of all the patterns are the same, except for between Sr and Nb. Units 9 and 11 do seem to be different than the other units, particularly with respect to the more incompatible elements; they are also two of the three samples that contain *ol* but no *q*.

Variance From MORB

Tholeiitic basalts from Site 907 are similar to N-MORBs, but a variety of trace- and major-element abundances differ compositionally from N-MORBs. The tholeiites have major element concentrations similar to N-MORB with the exception of K₂O, Al₂O₃, and TiO₂. The extremely low K₂O contents for six of the eight samples (Table 3) are most similar to N-MORBs; however, Units 9 and 11 have much higher K₂O, similar to P-MORBs/E-MORBs (Schilling et al., 1983). TiO₂ contents are higher than is typical of MORB compositions and Al₂O₃ is lower; both oxides are more similar in abundance to those of ocean island basalts (OIBs) (BVSP, 1981). K₂O/TiO₂ values (0.04–0.16, Table 3), are most similar to N-MORB K₂O/TiO₂ (≈ 0.06), but Units 9 and 11 still have higher K₂O and therefore higher K₂O/TiO₂ values, approaching those for E-MORB (0.25) (Floyd, 1991).

Trace-element abundances vary, but many are closer to E-MORB compositions than N-MORB. For example, Nb values range from 6.6 to 7.8 ppm for the Site 907 basalts; average N-MORB contains 2.33 ppm and average E-MORB contains 8.3 ppm (values from Floyd,

Table 3. Major-element compositions of Leg 151 basalt samples, Site 907.

	Unit 2	Unit 3	Unit 5	Unit 6	Unit 9	Unit 10	Unit 11	Unit 12
151-907A-:	25X-1,	25X-1,	25X-2,	25X-2,	26X-1,	26X-1,	26X-2,	26X-2,
Interval (cm):	13–16	81–84	22–26	73–77	35–38	85–89	6–11	56–59
SiO ₂	51.8	50.8	49.4	51.2	49.5	49.9	49.3	51.4
TiO ₂	1.94	1.92	1.88	1.86	1.78	1.85	1.80	1.86
Al ₂ O ₃	14.2	13.9	13.8	13.6	13.1	13.3	13.2	13.8
FeO*	13.3	13.7	14.7	14.3	15.4	14.9	16.1	13.8
MnO	0.18	0.19	0.23	0.21	0.26	0.22	0.23	0.19
MgO	6.25	7.09	7.07	6.37	6.89	7.13	6.98	6.90
CaO	9.59	9.77	10.4	10.2	10.6	10.2	9.71	9.67
Na ₂ O	2.47	2.32	2.26	2.07	2.08	2.22	2.23	2.18
K ₂ O	0.12	0.07	0.07	0.09	0.21	0.05	0.28	0.10
P ₂ O ₅	0.19	0.18	0.12	0.19	0.18	0.18	0.20	0.17
K ₂ O/TiO ₂	0.06	0.04	0.04	0.05	0.12	0.03	0.16	0.05
Orig. sum	100.5	100.4	100.1	99.8	99.8	99.9	99.9	99.4
mg	46	48	46	46	44	46	44	46

CIPW normative analyses (Fe ₂ O ₃ as 0.10 × FeO _{Total})								
q	3.55	1.84		3.70		0.39		3.35
or	0.71	0.41	0.41	0.53	1.24	0.30	1.65	0.59
ab	20.9	19.6	19.1	17.5	17.6	18.8	18.9	18.4
an	27.3	27.3	27.3	27.6	25.8	26.2	25.2	27.6
di	15.8	16.6	19.6	18.2	21.4	19.3	18.1	16.0
hy	25.7	28.1	25.5	26.6	27.3	28.9	27.0	28.2
ol			2.03		0.68		3.04	
mt	1.93	1.99	2.13	2.07	2.23	2.16	2.33	2.00
il	3.68	3.65	3.57	3.53	3.38	3.51	3.42	3.53
ap	0.44	0.42	0.28	0.44	0.42	0.42	0.46	0.39

Note: mg = 100 × Mg/(Mg + Fe). Analyses have been normalized to 100 wt% (volatile-free basis) and then rounded off for standard presentation. Original sums (Orig. sum) are presented.

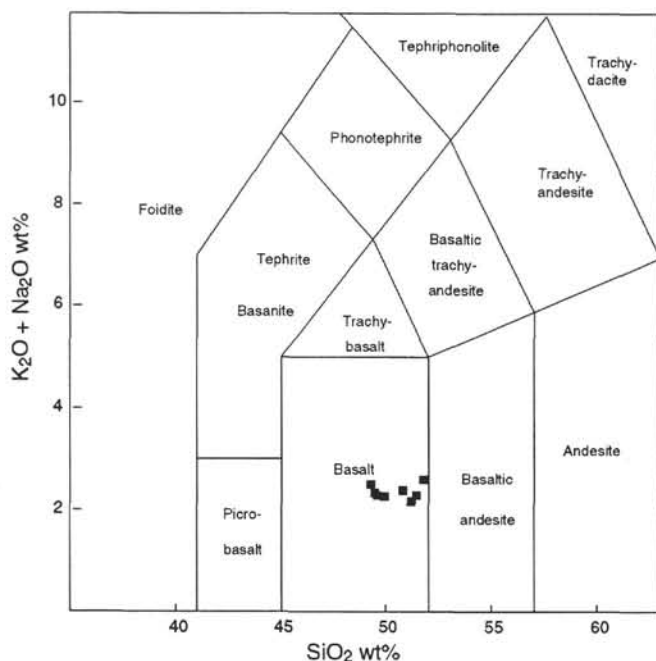


Figure 4. Total-alkali silica diagram using the I.U.G.S. classification scheme (Le Bas et al., 1986). Solid squares are averaged XRF analyses from Site 907, normalized to 100% without volatiles.

1991). For Cr, Cs, Nb, Ni, and the LREE, where a significant difference exists between N-MORB and E-MORB, the Site 907 basalts are closest to E-MORB compositions (Table 4; compared to values from Sun and McDonough, 1989). For Rb, Sc, Sr, and the HREE, the Site 907 basalts are closest to N-MORB compositions (Table 4). The range in each of the ratios can vary a great deal. For example, Hf/Th

ranges from 5.6 to 11.3, P/Ce ranges from 19 to 32, K/Rb ranges from 145 to 249, and Hf/Lu from 4.0 to 5.2. K₂O/TiO₂ variance is similar and was discussed above. Trace element ratios also vary between being more similar to N-MORB or to E-MORB. Some examples of ratios varying from typical E-MORB to N-MORB follow. La/Nb of 0.6 to 0.7 is closer to E-MORB (0.8) than N-MORB (1.1); K/Rb of 145 to 249 is much closer to E-MORB (415 vs. 1067 of N-MORB); Hf/Th of 11–6 bridges the gap (N-MORB has 17.08 and E-MORB has 3.4); La/Nb of 0.6 to 0.7 is closer to 0.76 of E-MORB than 1.1 of N-MORB. So far, no real pattern has emerged.

⁴⁰Ar/³⁹Ar DATING

The area of the Iceland Plateau on which Site 907 is located has a complicated tectonic history. The plateau is in an area where seafloor spreading is asymmetric, where ridge-jumping has occurred more than once, and where most magnetic anomalies are poorly identified (Talwani and Eldholm, 1977). Anomalies 5A to 6C on the Iceland Plateau are the most recognizable anywhere in the Atlantic and allowed Vogt et al. (1980) to pinpoint a late Tertiary plate acceleration at 12–14 Ma. Site 907 sits east of the present-day spreading ridge but west of the ridge some have considered to be an extinct spreading axis. The nearest drill hole where basalt has been recovered is Site 348, Leg 38 (Talwani, Udintsev, et al., 1976), which sits on the opposite side of the extinct ridge and south of Site 907. The basalt from Site 348 has a K-Ar age of about 19 m.y. (Kharin et al., 1976). The age of the basalts at Site 907 could be a very valuable tool in unraveling the tectonic and magmatic history of the area.

Sample Description

The specimens were chosen from the interior of Units (pillows) 3, 6, and 10, as close as possible to sections of the core that had been analyzed microscopically in thin section and chemically (Table 3); in each case, samples for ⁴⁰Ar/³⁹Ar analysis were taken from the same pillow as the nearby previously analyzed samples. The samples cho-

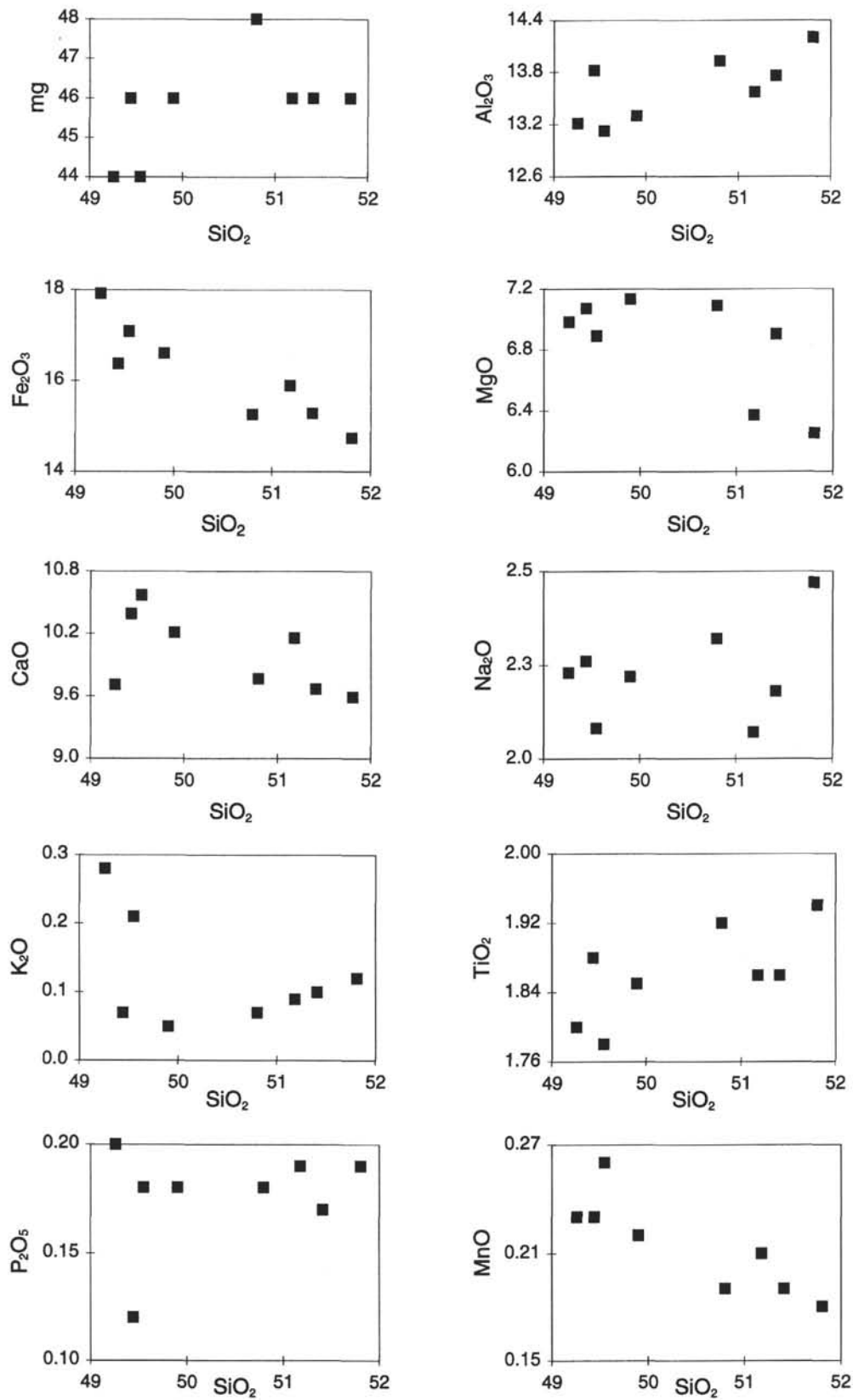


Figure 5. Whole-rock major-element compositions of Site 907 basalts.

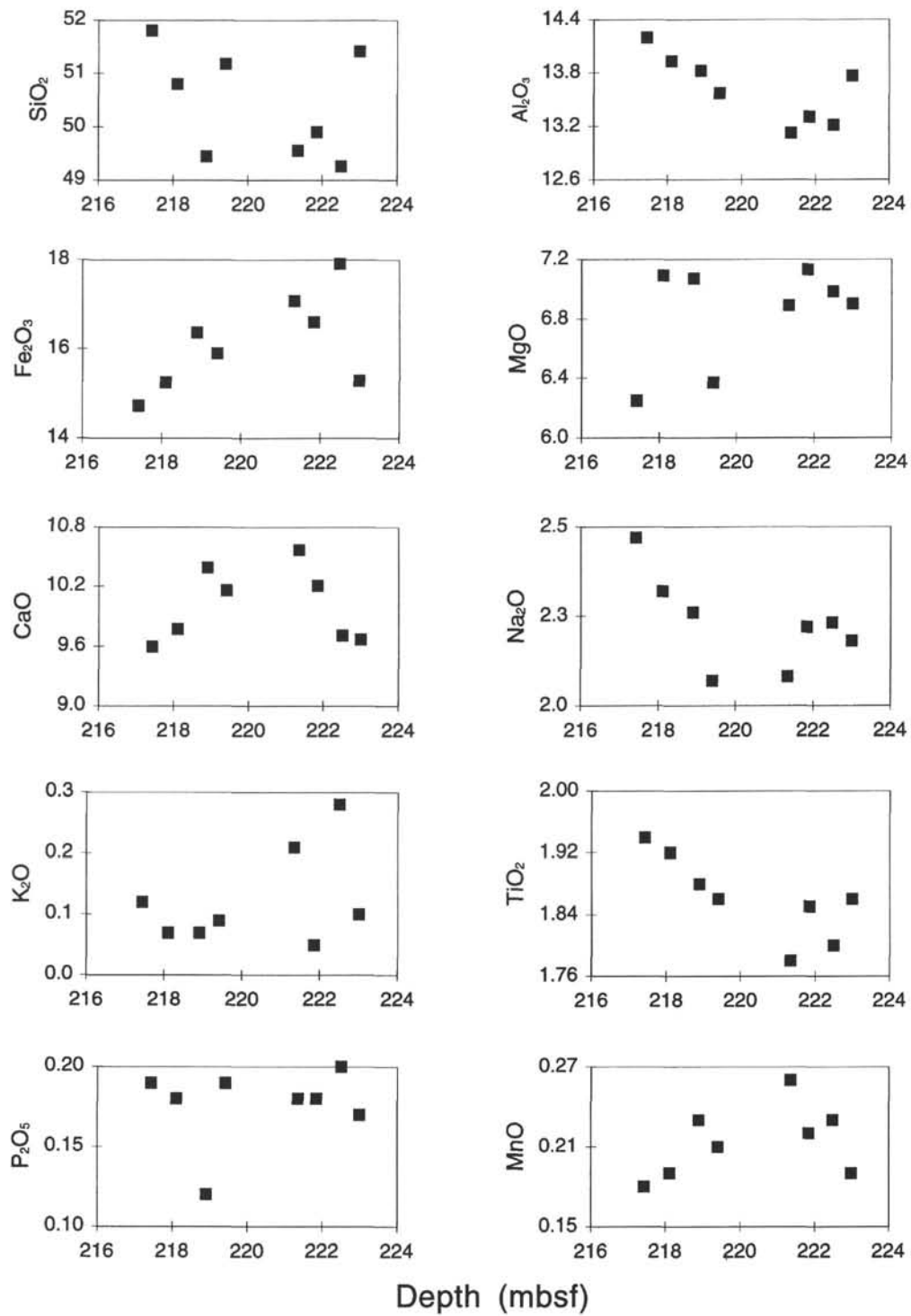


Figure 6. Change in basalt composition with depth of Hole 907.

Table 4. Trace-element compositions of Leg 151 basalt samples, Site 907.

Interval (cm):	Unit 2		Unit 3		Unit 5		Unit 6		Unit 9	Unit 10		Unit 11
	8-13	13-16	81-84	85-89	22-26	26-32	73-77	76-82	35-38	72-77	85-89	6-11
Sc	54.5			53.3		53.1		53.6		52.3		55
V		505	521		484				480		493	482
Cr	73			67		72		70		70		66
Co	78			60		65		70		61		
Ni		48	43		54				45		40	36
Cu		117	112		108				106		110	96
Zn		137	147		142				126		138	128
Ga		18	17		19				21		20	20
As	1			1		1				4		
Br	4.4			4.3		4.4		4.4		3		
Rb		2	0		0				6		0	8
Sr		73	67		68				66		64	66
Y		46	48		49				48		49	47
Zr		97	98		96				93		95	93
Nb		7.2	6.6		6.6				7.5		6.5	7.8
Cs				0.5								
La	4.5			4.6		4.4		4.5		4.2		
Ce	13			13		14		13		13		
Nd	10			11		10		11		10		
Sm	3.88			3.94		3.95		3.93		3.78		
Eu	1.28			1.65		1.23		1.55		1.54		
Tb	1.1			1.1		1.2		1.2		1.2		
Yb	4.43			4.65		5.06		4.84		4.51		
Lu	0.66			0.72		0.76		0.69		0.69		
Hf	3.4			3.3		3.3		3.4		2.8		
Pb					3							
Th	0.3			0.3						0.5		
U	0.4					0.4		0.5				
Nd/Sm	2.6			2.8		2.5		2.8		2.6		
Zr/Hf	28.5			29.7		29.1				33.2		
Hf/Th	11.3			11.0						5.6		
La/Tb	4.1			4.2		3.7		3.8		3.5		
La/Ce	0.35			0.35		0.31		0.35		0.32		
Hf/Lu	5.2			4.6		4.3		4.9		4.0		
La/Nb	0.63			0.70		0.67				0.56		

Notes: Elements determined by INAA include: Sc, Cr, Co, As, Br, Cs, REEs, Th, and U. Elements determined by XRF include: V, Ni, Cu, Zn, Ga, Rb, Sr, Y, Zr, Nb, and Pb. Values are in ppm.

seen from the recovered core were those that showed the least alteration. Complete thin section descriptions are in Myhre, Thiede, Firth, et al. (1995). Brief sample descriptions follow here so that the reader may fully evaluate the degree of alteration of the basalts and therefore evaluate the age of the basalt presented. All are of tholeiitic olivine basalts, sampled in the center of pillows away from glassy rims and vesicular rinds. Sample 151-907A-25X-1, 85-89 cm, Piece 11, also sampled for thin section and chemical analysis at 81-84 cm, ranges from glassy to 2.0 mm in grain size. The textures are subophitic to microporphyritic and quenched. Plagioclase and pyroxene phenocrysts or microphenocrysts to 2.0 mm in size are present, and the groundmass contains plagioclase, pyroxene, and opaque minerals. Olivine and glass were perhaps initially present but are now altered. Secondary mineralogy includes pyrite, unknown brown minerals, sericite, chalcedony and an unknown mineral(s) that replaces clinopyroxene. Sample 151-907A-25X-2, 76-82 cm, Piece 7B, overlapping with a piece of the core sampled for thin section and XRF analysis at 73-77 cm, is also glassy to 2.0 mm in grain size. Textures are microglomeroporphyritic, subophitic, quenched, and variolitic. Plagioclase and pyroxene microphenocrysts are present, and the groundmass contains plagioclase, clinopyroxene, and opaque minerals. Olivine and glass may have been present as indicated by alteration products and "ghosts." Alteration products or secondary minerals include pyrite, chalcedony, a brown clay mineral, and an unknown mineral(s) replacing clinopyroxene. Sample 151-907A-26X-1, 72-77 cm, Piece 10B, as close a piece as possible to Piece 11A, 85-89 cm, which was analyzed previously, is the only sample with a $^{40}\text{Ar}/^{39}\text{Ar}$ analysis that is probably accurate and that is reported here. This sample has a grain size that ranges from glassy to 1.0 mm. Textures are microporphyritic, subophitic, and variolitic. Clinopyroxene

and plagioclase are the microphenocrysts present, and it appears that olivine may also have been a phenocryst phase. What may have been olivine is now replaced by brown clay minerals or mineraloids. The groundmass contains plagioclase, clinopyroxene, and opaque minerals. Glass and olivine may have been present in the groundmass initially. Secondary minerals include pyrite, brown clay minerals, sericite, and chalcedony.

Results

Results from Sample 151-907A-25X-2, 76-82 cm, Piece 7B, were discounted because of a very disturbed spectrum and negative radiogenic yields. Results from Sample 151-907A-25X-1, 85-89 cm, Piece 11, were discounted mostly because of relatively high radiogenic Ar yield above 900°C suggestive of zeolites or chert releasing trapped Ar, and because of climbing spectra above the same temperature.

$^{40}\text{Ar}/^{39}\text{Ar}$ age spectra and data (along with % radiogenic argon, K/Ca, and Cl/K for each temperature increment), for Sample 151-907A-26X-1, 72-77 cm, Piece 10B, are presented in Figure 9 and in Table 5. We regard this $^{40}\text{Ar}/^{39}\text{Ar}$ data as tentative and we are in the process of trying to duplicate the determined age. We have presented data for each of the heating increments to show the consistency of the low-temperature steps. The lower temperature spectra give younger ages, while the higher temperature ages range up to 24 Ma. The integrated age of all heating steps, equivalent to a conventional K-Ar age, is 19.7 Ma. The best estimate of the eruption age of this sample is represented by the isochron of the low-temperature heating steps (Table 5; Fig. 10). This isochron, which is well correlated and has an atmospheric intercept, gives an age of 13.2 ± 0.3 Ma. This age is consid-

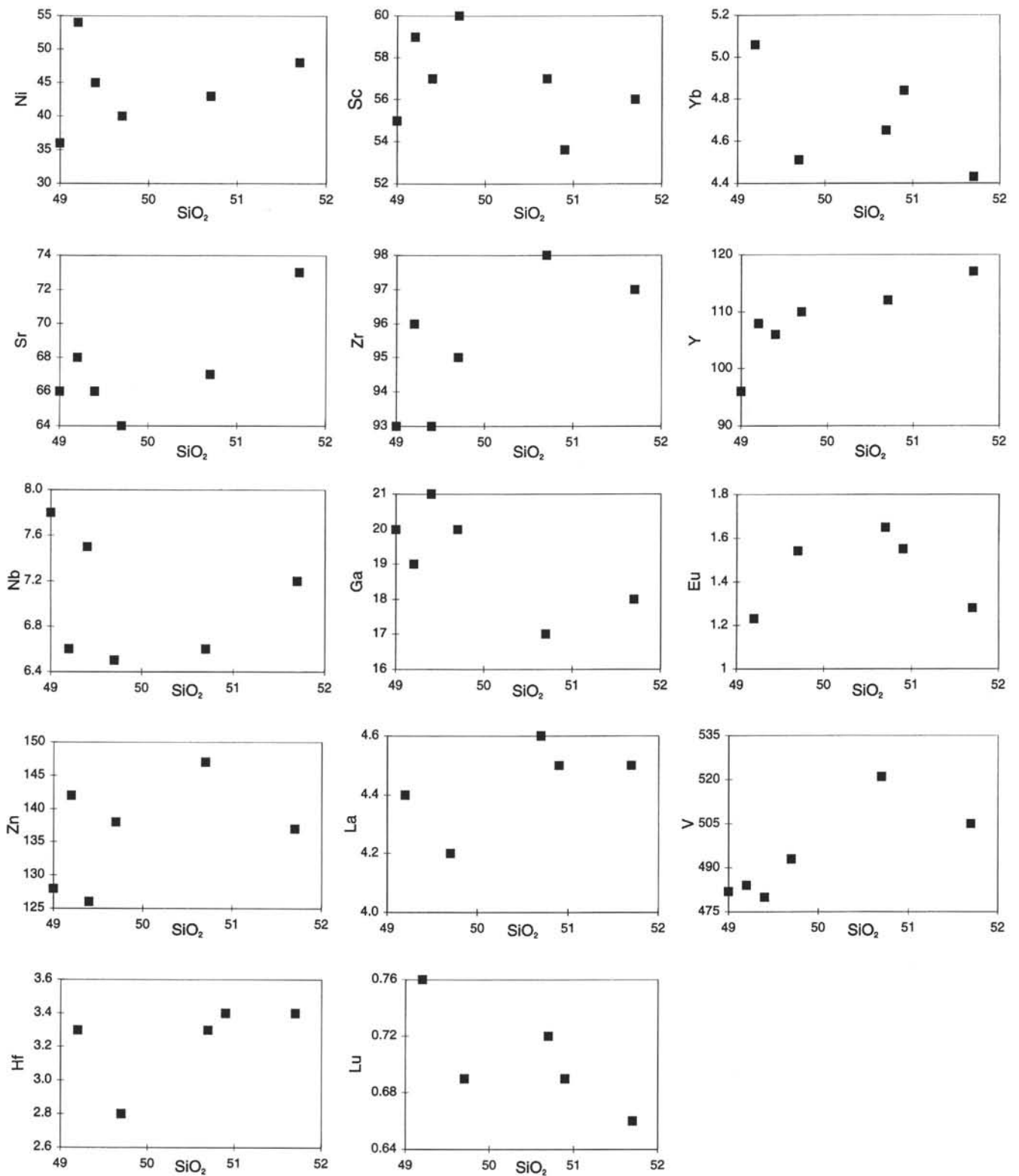


Figure 7. Whole-rock trace-element compositions of Site 907 basalts.

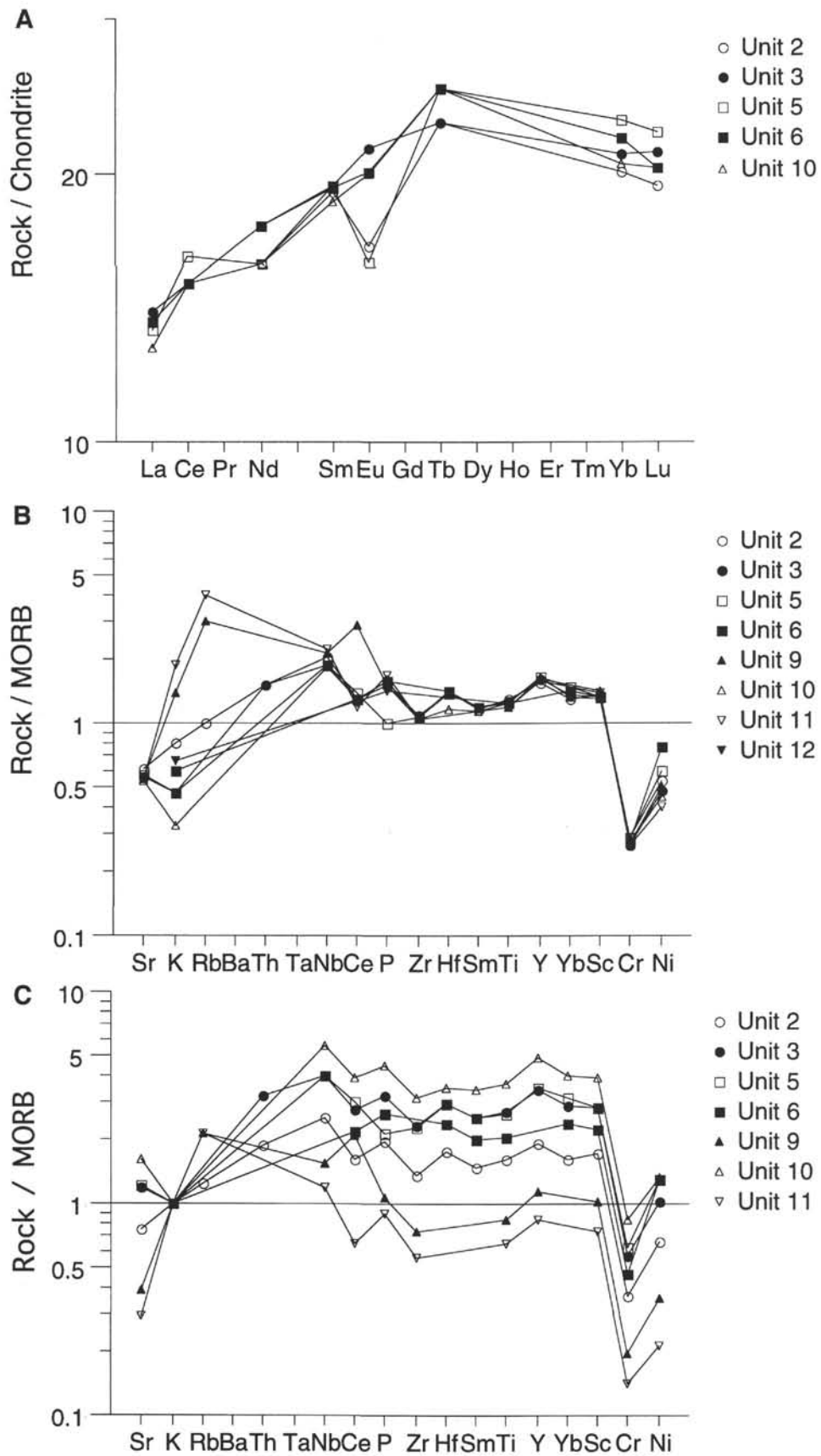


Figure 8. Spider diagrams for (A) chondrite-normalized REE, (B) MORB-normalized incompatible element plot double-normalized to $K = 1$. Diagrams plotted using Spider (Wheatley and Rock, 1988). Chondrite values (C1) are from Thompson et al. (1984) and MORB values are those used by Wheatley and Rock (1988) in their plotting program.

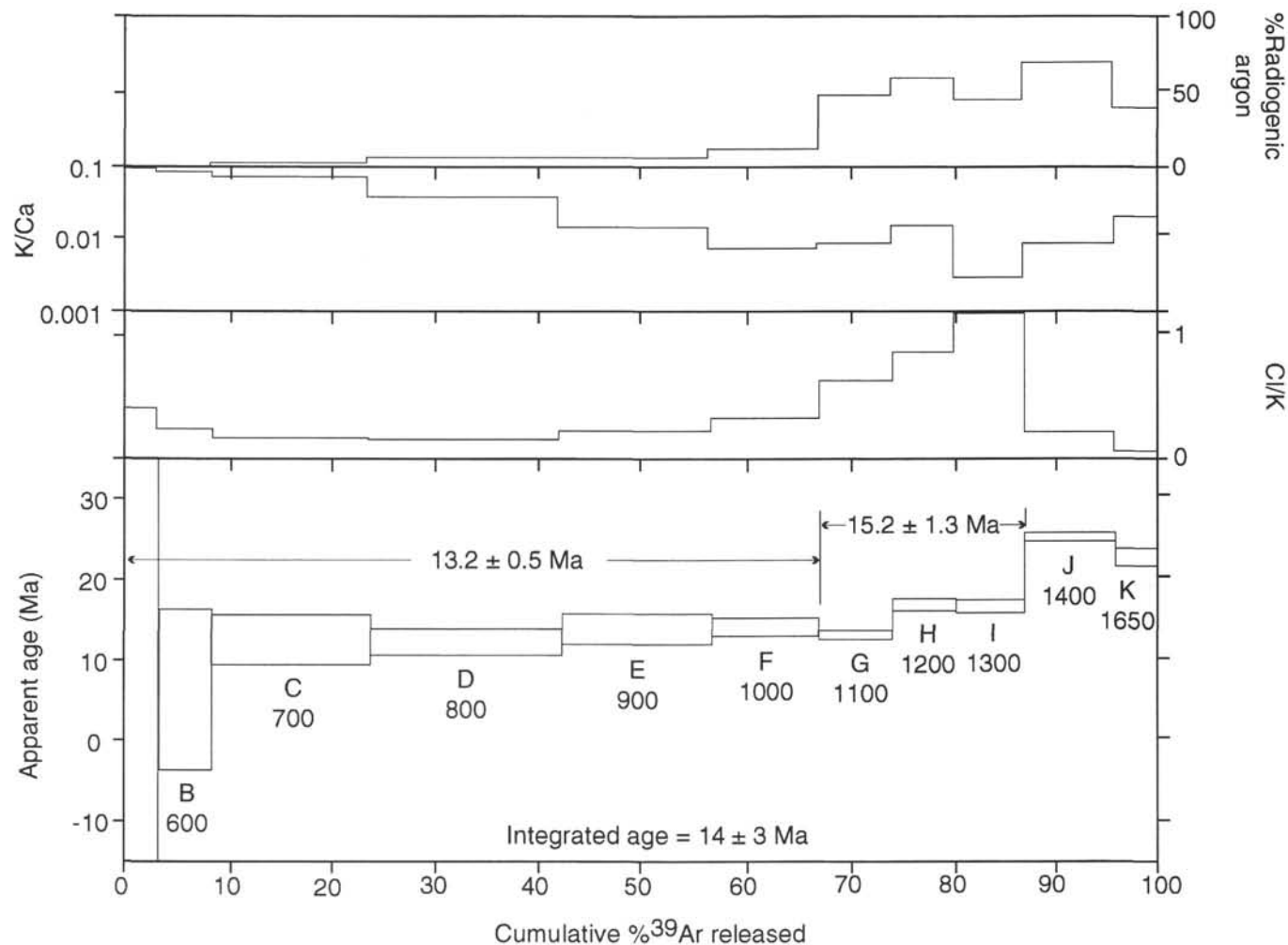


Figure 9. $^{40}\text{Ar}/^{39}\text{Ar}$ age spectra for Sample 151-907A-26X-1, 72-77 cm, Piece 10B. Incremental heating steps (B-K) are shown with temperatures ($^{\circ}\text{C}$).

Table 5. Summary of $^{40}\text{Ar}/^{39}\text{Ar}$ data.

Summary of spectra for Sample 151-907A-26X-1, 72-77 cm, Piece 10B											
Run	T ($^{\circ}\text{C}$)	$^{40}\text{Ar}/^{39}\text{Ar}$	$^{37}\text{Ar}/^{39}\text{Ar}$	$^{36}\text{Ar}/^{39}\text{Ar}$	^{39}K (moles)	K/Ca	Cl/K	$\%^{40}\text{Ar}^*$	$\%^{39}\text{Ar}^*$	Age (m.y.)	\pm Error (m.y.)
1832-1A	500	2.26E+3	5.35E+0	7.63E+0	1.7E-16	9.5E-2	4.0E-2	0.4	3.40	11.2	34.2
1832-1B	600	7.61E+2	5.73E+0	2.56E+0	2.8E-16	8.9E-2	2.3E-2	0.6	8.97	6.4	10.1
1832-1C	700	2.90E+2	7.16E+0	9.53E-1	7.6E-16	7.1E-2	1.7E-2	3.1	24.29	12.5	3.0
1832-1D	800	1.55E+2	1.33E+1	4.98E-1	9.3E-16	3.8E-2	1.3E-2	5.7	43.17	12.3	1.5
1832-1E	900	1.72E+2	3.71E+1	5.60E-1	7.2E-16	1.4E-2	2.1E-2	5.6	57.82	13.7	1.9
1832-1F	1000	8.71E+1	7.00E+1	2.80E-1	5.1E-16	7.3E-3	3.2E-2	11.1	68.13	14.1	1.2
1832-1G	1100	1.93E+1	6.11E+1	5.04E-2	3.4E-16	8.4E-3	6.1E-2	47.2	75.05	13.2	0.5
1832-1H	1200	2.00E+1	3.62E+1	3.70E-2	3.0E-16	1.4E-2	8.5E-2	59.2	81.13	16.8	0.6
1832-1I	1300	2.36E+1	1.88E+2	9.33E-2	3.1E-16	2.7E-3	1.3E-1	44.1	87.30	16.5	0.7
1832-1J	1400	2.45E+1	6.51E+1	4.17E-2	4.2E-16	7.8E-3	1.9E-2	70.0	95.73	24.8	0.5
1832-1K	1650	4.18E+1	2.77E+1	9.49E-2	2.1E-16	1.8E-2	4.3E-3	38.0	100.00	22.3	1.0
Total gas age									n = 11	14.1	3.1
Mean of low-temperature steps									n = 7	13.2	0.5
Mean of high-temperature steps									n = 3	15.2	1.3
Isochron age (low-temperature steps)									n = 6	13.2	0.3
Isochron age (all steps)									n = 11	19.7	0.1
J = 0.0007683 \pm 0.0000002											

Summary of $^{40}\text{Ar}/^{39}\text{Ar}$ results for Sample 151-907A-26X-1, 72-77 cm, Piece 10B									
Groupings	Spectrum age (m.y.)			Isochron age (m.y.)					
	n	Age	Error	n	Age	Error	MSWD	$^{40}\text{Ar}/^{36}\text{Ar}$	Error
Low-temperature steps	7	13.2	0.5	6	13.2	0.3	0.4	295.2	1.2
High-temperature steps	3	15.2	1.3	—	—	—	—	—	—
All steps	—	—	—	11	19.7	0.1	191.4	288.5	1.1

Note: — = not determined.

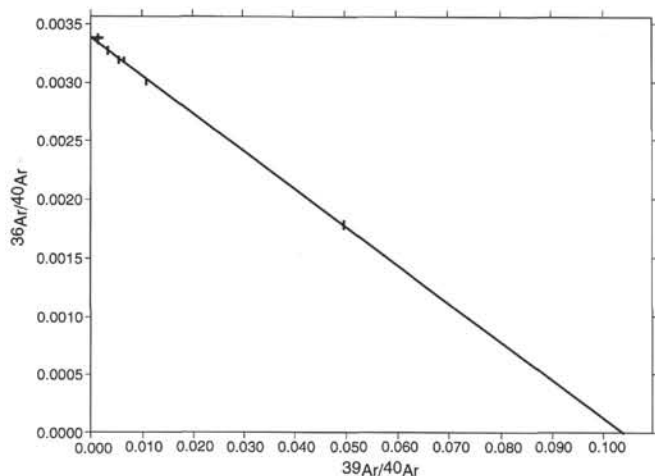


Figure 10. Isochron for Sample 151-907A-26X-1, 72-77 cm, Piece 10B.

ered to be relatively accurate, although the very low MSWD value of 0.4 reflects imprecision of the analysis due to low potassium content and low radiogenic yields.

DISCUSSION

Tholeiitic basalts from the Iceland Plateau at Site 907 are not primitive, and the parent magmas most likely suffered crystal fractionation. Pillows are plagioclase and augite phyric, accompanied by rare olivine that is now completely altered. The basalts are evolved as indicated by the rarity of olivine, the absence of spinel, and the abundance of augite and ilmenite accompanied by pigeonite. Microphe-nocrysts are not embayed, but they are frequently euhedral and were probably in equilibrium with the equivalent melt. Chondrite-normalized REE patterns with small Eu-depletions are indicative of plagioclase fractionation. Trace-element patterns normalized to typical N-MORB values with relative depletions in Cr, Ni, and Sr, could reflect source characteristics or more likely be indicative of fractionation of plagioclase and clinopyroxene (Sr, spinel, or olivine (Cr and Ni)).

The evolved nature of the basalts is also indicated by whole-rock major element composition. They range in composition almost to basaltic andesites and have very low Mg numbers (≈ 46). MORB with mg numbers this low are generally uncommon in the Atlantic Ocean and are also uncommon with respect to all MORB (Wilkinson, 1982). However, the evolved nature of these basalts and their quartz-normative character is in agreement with the earlier findings of unusually evolved basalt glasses from the Kolbeinsey Ridge (Sigurdsson, 1981). In addition, the Iceland Plateau basalts are strikingly similar to some of the Group A basalts from the Reykjanes Ridge, the western zone of Iceland, and the Kolbeinsey Ridge described by Sigurdsson (1981) in two ways. First, they contain pigeonite or low-Ca pyroxene, and that although in some cases entire grains are Ca-poor, usually a Ca-poor or pigeonite core is enclosed in a Ca-rich rim. Second, the range in pyroxene composition is also from augite to Ca-poor pyroxene or pigeonite and spans an area of the pyroxene quadrilateral that is generally referred to as the "forbidden zone"; however, this is characteristic of quenched pyroxenes in quenched basalts (Muir and Tilley, 1964).

The pillow basalts are almost uniformly fine grained and glassy, indicating rapidly quenched volcanic liquids, thus, variation diagrams based on rock analyses may truly characterize the magmatic lineage. It is very difficult to interpret the "trends" illustrated by Harker variation diagrams (Figs. 5-7). As discussed, the small num-

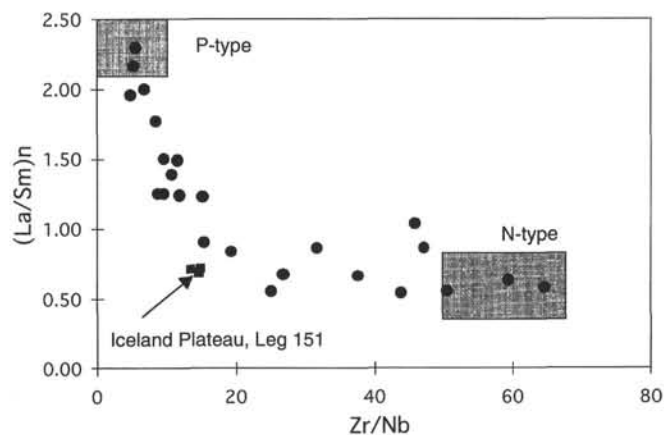


Figure 11. Chondrite-normalized La/Sm compared to Zr/Nb for Iceland Plateau basalts at Site 907 and MORB from the Atlantic, Pacific, and Indian Oceans. Modified after Wilson (1988).

ber of samples may be reflected in the scatter; if a larger data base existed, better straight-line trends might emerge. Some degree of alteration may explain some of the major-element variation, but it cannot explain the trace-element variation. We cannot discount more than one magma source which could lead to the patterns seen. This would not be unusual given the possibility that a large number of small magma chambers may exist below the ridge or the extinct ridge (c.f. Smith and Cann, 1993), and given the distinct break in the layer(s) of pillow basalt at 220 m (Fig. 6).

The variation in major- and trace-element compositions and trace-element ratios provide strong evidence for magma mixing. The nature of the proposed magma mixing is unknown. Variation in trace-element ratios is indicative of different sources and the lack of good linear trends in the Harker variation diagrams supports a theory of more than one source for the basalt. It may be that different mantle sources are or were present at the time of magma generation, but equally possible is that magma was tapped from different depths in the magma column as discussed by Devey et al. (1994) and Elliot et al. (1991). Even if different magma chambers containing melts with the same or similar sources were tapped, the melts in these chambers being more or less evolved still would not have different trace-element ratios, unless the melts came from different depths of a melting column. The large range in trace-element ratios such as K_2O/TiO_2 (0.04-0.16) or Hf/Th (5.6-11.3) in the Site 907 basalts is similar to although sometimes greater than or less than, ranges in ratios discussed by Devey et al. (1994).

The tholeiitic basalts on the Iceland Plateau at Site 907 are transitional MORBs (T-MORB), but just barely. Major- and trace-element signatures fall most often between N-MORB and E-MORB/P-MORB. Trace-element ratios also show this dual signature (Fig. 11). MORB compositions from the Atlantic, Pacific, and Indian Oceans form a mixing curve from plume-type or enriched MORB to normal MORB. Schilling et al. (1983) subdivided the Mid-Atlantic Ridge into three segments: "normal ridge segments" characterized by $(La/Sm)_n$ less than 0.7; "plume segments" characterized by $(La/Sm)_n$ maxima; and "transitional ridge segments" characterized by large scale gradients in $(La/Sm)_n$ (e.g., 0.7-1.8) adjacent to plume segments. Samples from Site 907 plot at neither end-point of the mixing curve but almost directly between the two, with low Zr/Nb and $(La/Sm)_n$ of 0.68-0.72. It is important to note that the "plume segment" that these transitional basalts are near is not the Iceland plume, but may be the hypothesized plume at Jan Mayen. Mertz et al. (1991) have presented convincing isotopic evidence that an Iceland component is not an end-member in the source(s) of the southern Kolbein-

sey Ridge basalts. However, the portion of the ridge north of the Spar fracture zone (at about 69°N) appears to be from a different geochemical province showing higher Pb and Sr isotope ratios and higher La/Sm ratios than samples from the southern Kolbeinsey Ridge (Mertz et al., 1991). Site 907 is north of the Spar fracture zone. The data of Schilling et al. (1983) also show increasing (La/Sm)_n from the Spar fracture zone to Jan Mayen.

The ⁴⁰Ar/³⁹Ar data may be in agreement with paleontological and paleomagnetic interpretations and data. There is no firm evidence to provide disagreement. Sediments near the bottom of Hole 907A (187.85 mbsf) are estimated to be ~14.164 Ma from paleomagnetic data; however, several significant hiatuses below 150 mbsf make correlation of the magnetozones to the geomagnetic polarity time scale of Cande and Kent (1992) rather uncertain (Shipboard Scientific Party, 1995). Paleontological data is in general agreement about the age of the sediments in the bottom of Hole 907A being Middle Miocene, with the possible exception of diatoms. Diatoms may indicate an age in the early part of the Middle Miocene; however, diatom ages are calibrated to the magnetostratigraphy from Leg 104 (Eldholm, Thiede, Taylor, et al., 1987), which is somewhat controversial.

All three samples analyzed yielded climbing age spectra with low-temperature, low radiogenic yield initial steps, followed by higher yield steps of increasing age. The low radiogenic yields (0.6%–47%), unusually low for basalts of about 10 Ma, probably reflect atmospheric Ar trapped in alteration phases, possibly zeolite or clay minerals. The discordant ages of higher temperature steps (10–25 m.y. older than low-temperature steps) probably reflect excess Ar in retentive phases, possibly plagioclase microphenocrysts. An alternative explanation is that the rocks are older than 13.2 Ma (i.e., 24 Ma), but were altered 10 m.y. after emplacement. This does not seem to fit with what we know about hydrothermal alteration of the seafloor. If the basalts were emplaced at 24 Ma, it is unlikely that hydrothermal alteration would occur 10 m.y. later to produce the low-temperature spectra we see, unless a second heat source were present. We have no evidence to suggest a second event, and it is more likely that the younger age of 13.2 Ma is accurate.

If the age presented here is indeed accurate, it is still difficult to determine the significance of the age with respect to plate tectonic arguments. Although the basalts dated herein are pillow basalts and undoubtedly erupted into water, it is in no way obvious that these basalts sampled represent acoustic basement. As discussed in Shipboard Scientific Party (1995), an opaque, extremely smooth acoustic basement reflector is characteristic of the Iceland Plateau, with short, indistinct reflector elements lying below this smooth reflector. The basalts drilled at Site 907 came from the upper smooth reflector. It was suggested by Eldholm and Windish (1974) that the true oceanic basement of the Iceland Plateau is below the smooth reflector. Basalt drilled at Site 348, Leg 38 (Talwani, Udintsev, et al., 1976) near Site 907, appears to be from the same smooth reflector; it was sampled and dated by K-Ar analysis at 18.8 ± 1.7 m.y. (Kharin et al., 1976). Neither pillow structures nor glassy rims were found in the basalts at Site 348, and it may be that the basalt is from a major sill-like body; however, Kharin et al. (1976) argue that the basalts at Site 348 are not necessarily intrusive. Note that the integrated ⁴⁰Ar/³⁹Ar age of 19.7 Ma reported here is within experimental error of Kharin et al.'s (1976) K-Ar age. As discussed in Shipboard Scientific Party (1995), Site 907 was drilled on either Anomaly 6B crust, between 22 and 24 Ma (Talwani and Eldholm, 1977), or on crust of Anomaly 5B age, between 14 and 15 Ma (Vogt et al., 1980). The ⁴⁰Ar/³⁹Ar age presented here would seem to indicate that Site 907 sits on crust closer to Anomaly 5B. What is interesting to note here is that the age we have obtained, 13.2 Ma, correlates well with the time of plate acceleration between 12 and 14 Ma ago, discussed by Vogt et al. (1980) that they

have suggested may be connected to a magmatic pulse of global proportions.

REFERENCES

- Basaltic Volcanism Study Project (BSVP), 1981. *Basaltic Volcanism on the Terrestrial Planets*: New York (Pergamon Press).
- Cande, S.C., and Kent, D.V., 1992. A new geomagnetic polarity time scale for the Late Cretaceous and Cenozoic. *J. Geophys. Res.*, 97:13917–13951.
- Devey, C.W., Garbe-Schönberg, C.-D., Stoffers, P., Chauvel, C., and Mertz, D.F., 1994. Geochemical effects of dynamic melting beneath ridges: Reconciling major and trace element variations in Kolbeinsey (and global) mid-ocean ridge basalt. *J. Geophys. Res.*, 99:9077–9095.
- Eldholm, O., Thiede, J., Taylor, E., et al., 1987. *Proc. ODP, Init. Repts.*, 104: College Station, TX (Ocean Drilling Program).
- Eldholm, O., and Windisch, C.C., 1974. Sediment distribution in the Norwegian-Greenland Sea. *Geol. Soc. Am. Bull.*, 85:1661–1676.
- Elliot, T.R., Hawkesworth, C.J., and Grönvold, K., 1991. Dynamic melting of the Iceland plume. *Nature*, 351:201–206.
- Floyd, P.A. (Ed.), 1991. *Oceanic Basalts*: New York (Van Nostrand Reinhard).
- Fram, M.S., and Leshner, C.E., 1993. Geochemical constraints on mantle melting during creation of the North Atlantic basin. *Nature*, 363:712–715.
- Hooper, P.R., Johnson, D.M., and Conrey, R.M., 1993. Major and trace element analyses of rocks and minerals by automated X-ray spectrometry. *Washington State Univ., Geol. Dep., Open File Rep.*
- Kharin, G.N., Udintsev, G.B., Bogatkov, O.A., Dmitriev, J.I., Raschka, H., Kreuzer, H., Mohr, M., Harre, W., and Eckhardt, F.J., 1976. K/Ar age of the basalts of Norwegian-Greenland Sea Glomar Challenger, Leg 38 DSDP. In Talwani, M., Udintsev, G., et al., *Init. Repts. DSDP*, 38: Washington (U.S. Govt. Printing Office), 1101–1168.
- Le Bas, M.J., Le Maitre, R.W., Streckeisen, A., and Zanettin, B., 1986. A chemical classification of volcanic rocks based on the total alkali-silica diagram. *J. Petrol.*, 27:745–750.
- Macdonald, G.A., and Katsura, T., 1964. Chemical composition of Hawaiian lavas. *J. Petrol.*, 5:82–133.
- Mertz, D., Devey, C., Todt, W., Stoffers, P., and Hofmann, A., 1991. Sr-Nd-Pb isotope evidence against plume-asthenosphere mixing north of Iceland. *Earth Planet. Sci. Lett.*, 107:243–255.
- Muir, I.D., and Tilley, C.E., 1964. Basalts from the northern part of the rift zone of the Mid-Atlantic Ridge. *J. Petrol.*, 5:409–434.
- Myhre, A.M., Thiede, J., Firth, J.V., et al., 1995. *Proc. ODP, Init. Repts.*, 151: College Station, TX (Ocean Drilling Program).
- Robinson, P., 1980. The composition space of terrestrial pyroxenes: internal and external limits. In Prewitt, C.T. (Ed.), *Pyroxenes*. *Rev. Mineral.*, 7:419–494.
- Samson, S.D., and Alexander, E.C., 1987. Calibration of the interlaboratory ⁴⁰Ar–³⁹Ar dating standard, Mmhb-1. *Chem. Geol. (Isot. Geosci. Sect.)*, 66:27–34.
- Schilling, J.-G., Zajac, M., Evans, R., Johnston, T., White, W., Devine, J.D., and Kingsley, R., 1983. Petrologic and geochemical variations along the Mid-Atlantic ridge from 29°N to 73°N. *Am. J. Sci.*, 283:510–586.
- Shipboard Scientific Party, 1992. Site 504. In Dick, H.J.B., Erzinger, J., Stokking, L.B., et al., *Proc. ODP, Init. Repts.*, 140: College Station, TX (Ocean Drilling Program), 37–200.
- , 1995. Site 907. In Myhre, A.M., Thiede, J., Firth, J.V., et al., *Proc. ODP, Init. Repts.*, 151: College Station, TX (Ocean Drilling Program), 57–111.
- Sigurdsson, H., 1981. First-order major element variation in basalt glasses from the Mid-Atlantic Ridge: 29°N to 73°N. *J. Geophys. Res.*, 86:9483–9502.
- Smith, D.K., and Cann, J.R., 1993. Building the crust of the Mid-Atlantic Ridge. *Nature*, 365:707–715.
- Sun, S.-S., and McDonough, W.F., 1989. Chemical and isotopic systematics of oceanic basalts: implications for mantle composition and processes. In Saunders, A.D., and Norry, M.J. (Eds.), *Magmatism in the Ocean Basins*. *Geol. Soc. Spec. Publ. London*, 42:313–345.

- Talwani, M., and Eldholm, O., 1977. Evolution of the Norwegian-Greenland Sea. *Geol. Soc. Am. Bull.*, 88:969-999.
- Talwani, M., Udintsev, G., et al., 1976. *Init. Repts. DSDP*, 38: Washington (U.S. Govt. Printing Office).
- Thompson, R.N., Morrison, M.A., Hendry, G.L., and Parry, S.J., 1984. An assessment of the relative roles of crust and mantle in magma genesis: an elemental approach. *Philos. Trans. R. Soc. London A*, 310:549-590.
- Vogt, P.R., Johnson, G.L., and Kristjansson, L., 1980. Morphology and magnetic anomalies north of Iceland. *J. Geophys.*, 47:67-80.
- Wheatley, M.R., and Rock, N.M.S., 1988. A Macintosh program to generate normalized multi-element spidergrams. *Am. Mineral.*, 73:919-921.
- Wilkinson, J.F.G., 1982. The genesis of mid-ocean ridge basalt. *Earth Sci. Rev.*, 18:1-57.
- Wilson, M., 1988. *Igneous Petrogenesis: A Global Tectonic Approach*: London (Unwin Hyman).
- Wood, D.A., Joron, J.L., Treuil, M., Norry, M.J., and Tarney, J., 1979. Elemental and Sr isotope variations in basic lavas from Iceland and the surrounding ocean floor. *Contrib. Mineral. Petrol.*, 70:319-339.

Date of initial receipt: 1 July 1995

Date of acceptance: 11 January 1996

Ms 151SR-124